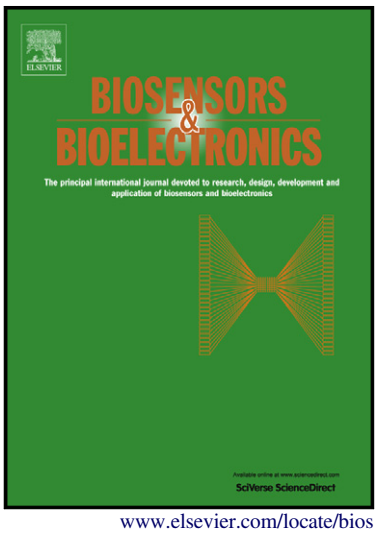

www.elsevier.com/locate/bios

Colorimetric surface plasmon resonance (SPR) imaging Biosensor Array based on polarization orientation rotation

Chi Lok Wong, George Chung Kit Chen, Xiaochao Li, Beng Koon Ng, Ping Shum, Peng Chen, Zhiping Lin, Chinlon Lin, Malini Olivo

PII: S0956-5663(13)00146-2
DOI: http://dx.doi.org/10.1016/j.bios.2013.02.040
Reference: BIOS5782

To appear in: *Biosensors and Bioelectronics*

Received date: 13 November 2012
Revised date: 6 February 2013
Accepted date: 22 February 2013

Cite this article as: Chi Lok Wong, George Chung Kit Chen, Xiaochao Li, Beng Koon Ng, Ping Shum, Peng Chen, Zhiping Lin, Chinlon Lin, Malini Olivo, Colorimetric surface plasmon resonance (SPR) imaging Biosensor Array based on polarization orientation rotation, *Biosensors and Bioelectronics,* http://dx.doi.org/10.1016/j.bios.2013.02.040

Colorimetric Surface Plasmon Resonance (SPR) Imaging Biosensor Array based on Polarization Orientation Rotation

Chi Lok Wong[a,b,c], George Chung Kit Chen[d], Xiaochao Li [e], Beng Koon Ng[b], Ping Shum[e], Peng Chen[f], Zhiping Lin[g], Chinlon Lin[h] and Malini Olivo[a, i*]**

[a]Bio-optical Imaging Group, Singapore Bioimaging Consortium, Helios #01-02, 11 Biopolis Way, Singapore 138667

[b]Division of Microelectronics, School of Electrical & Electronic Engineering, Nanyang Technological University, 50 Nanyang Drive, Singapore 639798

[c]Singapore Institute of Manufacturing Technology, 71 Nanyang Drive, Singapore 638075.

[d]BC Photonics Technological Co. 5255 Woodwards Rd., Richmond, B.C., Canada V7E 1G9.

[e]Division of Communication Engineering, School of Electrical & Electronic Engineering, Nanyang Technological University, 50 Nanyang Drive, Singapore 639798

[f]Division of Bioengineering, School of Chemical and Biomedical Engineering, Nanyang Technological University, 62 Nanyang Drive, Singapore 637459

[g]Division of Information Engineering, School of Electrical & Electronic Engineering, Nanyang Technological University, 50 Nanyang Drive, Singapore 639798

[h]Bell Labs and Bellcore, (Retired), Holmdel, NJ 07733, USA.

[i]School of Physics, National University of Ireland, Galway, Co. Galway, Ireland.

[*]Corresponding author at: Bio-optical Imaging Group, Singapore Bioimaging Consortium, Helios #01-02, 11 Biopolis Way, 138667, Singapore.

[**]Corresponding author.

Email: Malini_Olivo@sbic.a-star.edu.sg
Email: dave_wong@sbic.a-star.edu.sg
Email: clwongdave@yahoo.com.hk

Abstract

A colorimetric surface plasmon resonance (SPR) imaging biosensor array based on polarization orientation rotation is presented. It measures the spectral characteristic variations caused by the steep phase difference between the p- and s- polarization occurring at surface plasmon excitation and provides enhanced sensor resolution over existing SPR imaging sensors, while the two-dimensional (2D) sensing capability of the imaging sensor enables multiplex, high throughput array based simultaneous detection for a range of different bio-molecular interactions. Experiments on the binding interactions detection between anti-bovine serum albumin (anti-BSA) and BSA antigen have been performed with the system. The binding interactions occurred at all sensor sites in a 5 x 4 protein array were real-time monitored by the imaging sensor simultaneously. A sensor resolution of 8.26ng/ml (125pM) has been demonstrated, which is one-order of magnitude (12 times) better than the detection limit reported by existing phase-sensitive SPR imaging sensors in the literature, while no time-consuming phase modulation and

phase extraction processes are required. Furthermore, the optical colorimetric image read-out of the sensor is easy to be identified by the end users comparing to conventional intensity or phase information. The colorimetric SPR imaging biosensor array can find promising potential applications in microarray based clinical disease diagnosis, high throughput protein biomarkers screening and drug screening.

Highlights

► A multiplex colorimetric SPR biosensor array based on polarization orientation is presented. ► It measures the spectral variations caused by the steep phase change occurring at SPR. ► A sensor resolution of 8.26ng/ml (125pM) has been demonstrated. ► This value is 1 order of magnitude better than that reported by existing phase SPR imaging sensors. ► It is a 2-D, non-labeling, real-time and high sensitivity analytical detection platform.

Keywords

Surface plasmon resonance (SPR) imaging; Multiplex detection; Protein array; Non-labeling; Phase detection; Polarization orientation.

1. Introduction

Protein biomarkers have gained rapid increasing research interests in recent years (John et al., 2012; Lee et al., 2008; Surinova et al., 2011). Detection of the expression level of protein biomarkers in patient samples enables early disease diagnosis (Tomizaki et al., 2010; Shi et al., 2011) treatment response assessment (Bass et al., 2010; Peña et al., 2010). Haab *et al.* (Haab et al., 2001) demonstrated the application of antibody microarray for high throughput proteomics studies and antibody is by far the most widely used probe for biomarker profiling (Lee et al., 2008). In antibody microarray detection, in which fluorescent labeling, secondary antibodies or enzyme are required in the detection process. In antibody array detection, different fluorescently labeled molecules or secondary antibodies are required for of the each array elements. Large scale multiplexed measurements are therefore limited by the availability of corresponding fluorescent labels or secondary antibodies.

Surface plasmon resonance imaging (SPRI) (Rothenhausler et al., 1998; Yeatman et al., 1987) is a non-labeling detection alternative (Homola et al., 2008; Homola et al., 2005) and the two dimensional sensing capability of SPR imaging enables multiplex detection for the antibody array (Lee et al., 2006; Motoki et al., 2005; Wong et al., 2008; Wong et al., 2007). SPR imaging measures the refractive index changes associated with the antibody-antigen binding occurring at the gold sensing surface (Homola et al., 2006; Wong et al., 2007). Common SPR imaging systems are based on intensity modulation (Jordan et al., 1997; Lee et al., 2006; Motoki et al., 2005; Nelson et al., 1999). It measures the reflectivity variation (intensity change) of the reflected light from the attenuated Kretschmann total internal reflection surface. Kretschmann configuration is by far the most widely used method for surface plasmon excitation (Homola et al., 2008). When the momentum of the surface plasmon wave and the momentum of the evanescent wave of the incident light is match, the surface plasmon will be excited. The resonance condition varies with different characteristics of metal film, prism and dielectric medium and the reflectivity variation (intensity change) due to refractive index change at the dielectric medium is finally imaged with a charge-coupled device (CCD). The SPR imaging provides the unique advantage of high-throughput array detection. However, the major limitation of conventional intensity SPR imaging sensors is the limited sensor resolution (10^{-5} RIU) (Homola et al., 2005). Grigorenko and Nikitin *et al.* (Nelson et al., 1996) reported the phase jump phenomenon in surface plasmon resonance and the steep slope of the phase response provides ultra-sensitivity improvement. In the past decade, Interferometry based phase SPR imaging sensors have been intensively studied by different research groups (Ho et al., 2007; Lee et al., 2007; Wong et al., 2008; Wong et al., 2007; Yu et al., 2008; Yu et al., 2005). However, experimental findings show that interferometry based phase imaging methods are sensitive to environmental vibration and the signal to noise ratio is limited. In addition, complicated phase modulation and time-consuming fringe analysis are required in phase information extraction. Either part of the spatial or temporal domain information is necessary to be sacrificed in the phase modulation and extraction process. In recent years, spectral based SPR imaging sensor with the scanning of surface plasmon excitation minimum is reported (Yuk et al., 2008; Yuk et al., 2007; Yuk et al., 2003), however the sensor resolution is limited (10^{-5} RIU) and time-consuming scanning is required during measurement. In our previous research (Ho et al., 2006;

Wong et al. 2011; Wong et al., 2008; Wong et al., 2007; Wong et al., 2005), we imaged the color texture variations caused by the SPR absorption minimum shift and the system was applied to image the refractive index changes of lubricant at highly pressurized contact. Nevertheless, the sensor resolution is also limited.

In this paper, we report a colorimetric SPR imaging biosensor array based on the polarization orientation. It measures the spectral characteristic variation caused by the steep phase change occurring at surface plasmon excitation. A SPR prism coupler is placed in between two polarizers with perpendicular transmission axes and the transmission of incident beam is forbidden. At the excitation wavelength of surface plasmon, a phase difference is introduced between the p- and s- polarization component of the light. It rotates the orientation angle of the polarization ellipse and the light interacting with the surface plasmon is allowed to pass through the crossed polarizers setting. As the momentum of the surface plasmon wave only matches with particular wavelength range, particular spectral profile is produced, which is associated with the steep phase response at surface plasmon excitation. This method enhances the sensitivity of conventional spectral based SPR sensor through probing the steep phase response at surface plasmon resonance.

2. Materials and methods

2.1 Theory

Consider an elliptically polarized light *E* and the two orthogonal optical disturbances (p- and s-polarization) can be represented as (Eugene et al., 2001),

$$E_s = E_{0s}\cos(kz - \omega t) \qquad (1)$$

$$E_p = E_{0p}\cos(kz - \omega t + \varepsilon) \qquad (2)$$

where ε is relative phase different between the *p*- and *s*- polarization wave.

The elliptically polarized light *E* can further be described by the equation of an ellipse (Eugene et al., 2001),

$$\left(\frac{E_p}{E_{0p}}\right)^2 + \left(\frac{E_s}{E_{0s}}\right)^2 - 2\left(\frac{E_p}{E_{0p}}\right)\left(\frac{E_s}{E_{0s}}\right)\cos\varepsilon = \sin^2\varepsilon \qquad (3)$$

The principal axes of the ellipse make an orientation angle α with the (E_s, E_p) - coordinate system such that,

$$\tan 2\alpha = \left(\frac{2E_{0s}E_{0p}}{E^2{}_{0s} - E^2{}_{0p}} \right)\cos\varepsilon \quad (4)$$

Nelson *et al.* (Nelson et al., 1996) reported that there is a steep slope of phase response for the *p*-polarization light at surface plasmon excitation. However, the oscillation direction of the *s*-polarization light is perpendicular to the excitation plane of the surface plasmon wave and it is not affected at surface plasmon excitation (Homola et al., 2008; Homola et al., 2006; Wong et al., 2008; Wong et al., 2007). A phase difference $\Delta\phi$ is therefore produced between the p- and s-polarization light (Wong et al., 2008; Wong et al., 2007).

$$\Delta\phi = (\phi_p - \phi_s) \quad (5)$$

At surface plasmon resonance, the wave vector of *E* can be modified as

$$E_s{}' = E_{0s}\cos(kz - \omega t) \quad (6)$$

$$E_p{}' = E_{0p}\cos(kz - \omega t + \varepsilon + \Delta\phi) \quad (7)$$

The equation of the elliptically polarized light *E* and the orientation angle to the (E_s, E_p) - coordinate system are modified as

$$\left(\frac{E_p{}'}{E_{0p}}\right)^2 + \left(\frac{E_s{}'}{E_{0s}}\right)^2 - 2\left(\frac{E_p{}'}{E_{0p}}\right)\left(\frac{E_s{}'}{E_{0s}}\right)\cos(\varepsilon + \Delta\phi) = \sin^2(\varepsilon + \Delta\phi) \quad (8)$$

The principal axes of the ellipse now makes an orientation angle α' with the (E_s, E_p) - coordinate system (as described in Figure 1a) such that,

$$\tan 2\alpha' = \left(\frac{2E_{0s}E_{0p}}{E^2{}_{0s} - E^2{}_{0p}} \right)\cos(\varepsilon + \Delta\phi) \quad (9)$$

2.2 Experimental set-up

The experimental configuration of the polarization orientation based spectral SPR imaging sensor is described in Figure 1b. A halogen lamp is used as the board band light source. The beam is collimated by a lens set and the beam diameter is 50mm^2. The collimated beam incidents

on the total internal reflection surface of a glass prism. A gold sensing layer is coated on the prism surface through e-beam evaporation. In addition, a flow cell fabricated with polydimethylsiloxane (PDMS) materials is attached to the sensing surface for liquid samples handling during detection.

As described in Figure 1b, the SPR prism coupler is placed in between two polarizers with perpendicular transmission axes and the incident light is not allowed to transmit through. At (or close to) the excitation wavelength of the surface plasmon wave, a phase difference $\Delta\phi$ is introduced between the p- and s- polarization light. According to equation (9), the phase difference $\Delta\phi$ rotates the orientation angle of the elliptically polarized light E and it allows the light interacting with the surface plasmon to be transmitted through the crossed polarizers. At wavelength out of the excitation spectral range, the interaction between the incident light and the surface plasmon wave is weak and no significant transmitting light is recorded at the wavelength range longer or shorter than the surface plasmon excitation wavelength. The excitation wavelength changes according to the refractive index variation at the dielectric medium (Homola et al., 1999; Lam et al., 2005; Wong et al., 2005) and the shift of excitation wavelength eventually produces corresponding spectral profile variation. The color is changed with respect to the phase shift induced at surface plasmon resonance.

The spectral SPR image with phase information is finally captured by a CCD camera. A home-built MATLAB program has been developed for image analysis.

2.3 Surface chemistry

The gold sensing surface was immersed in ethanol containing 11-mercapto-undecanoic acid (MUA) (concentration-0.5mM, Sigma-Aldrich) for about 17 hours and a self-assembled monolayer (SAM) was formed on the gold surface. The modified surface was then rinsed by ethanol and distilled water. After that, the surface was activated with a mixture of N-hydroxysuccinimide (NHS) (concentration-1mM, Thermo Scientific) and 1-ethyl-3-(3-dimethylaminoprpyl) carbodiimide (EDC) (concentration-0.4mM, Thermo Scientific) in distilled water. The surface was rinsed with distilled water before the immobilization of protein samples. As described in Figure 1c, a protein array with bovine serum albumin (BSA, 2mg/ml in

phosphate buffered saline (PBS) buffer, Sigma-Aldrich) (positive sample), glucose oxidase (GOx, 2mg/ml in PBS, Sigma-Aldrich) (negative sample) and blank control sites (immersed with PBS buffer) was fabricated on the gold sensor surface for further experiment.

3. Results and discussion

The performance of the spectral SPR imaging sensor was characterized with different concentrations of salt solutions ranged from 0%, 1%, 2%, 3%, 4%, 5% to 7%, which corresponding to refractive index values from 1.3333 – 1.3454 RIU. The spectral SPR images are shown in Figure S1a-S1g. As shown in the results, the color of the SPR images change from red color (water) to green color (7% salt solution) and the green ingredient increases with increasing salt solution concentrations. The hue profiles of the SPR images were further extracted and the corresponding refractive index response curve of the imaging sensor is shown in Figure S-1f.

To demonstrate the two-dimensional, real-time and quantified detection capability of the spectral SPR imaging sensor for bio-molecular sensing applications, array based specific BSA antigen-antibody binding detections have been conducted. Figure 1c describes the configuration of the protein array fabricated for the experiment. Bovine serum albumin (BSA) sensor sites (red spots) are the specific samples and the glucose oxidase (GOx) sensor spots (black spots) serve as the non-specific sites in the experiment. The protein array also consists of four blank sensor sites (white spots), which indicate the non-specific binding occurring during the experiment. In the beginning of the experiment (0-30mins), the protein array was kept at PBS buffer solution. At 30 minutes, BSA antibody (2.5µl/ml in PBS) was injected to the protein array surface and the binding interactions were allowed to take place for 1 hour. At 91 minutes of the experiment, the array surface was washed with PBS buffer for the removal of non-specific bound molecules on the array surface. The whole binding processes occurred in all sensor sites were real-time monitored with the spectral SPR imaging sensor.

Figure 2 shows the spectral SPR images taken at different stages of the experiment. In Figure 2a, the protein array was kept in PBS buffer. Figure 2b and Figure 2c shows the spectral SPR images

taken at 15 minutes and 60 minutes after the BSA antibody injection (2.5µl/ml in PBS). As shown in the results, the color of the specific BSA antigen sites (A1, A4, B2, B3, C2, C3, D1, D4) changed from red (Figure 2a) to green color (Figure 2b) and the green color portion was increased against time. The color variations were caused by the refractive index variations associated with the binding interactions between BSA antigen-antibody molecules. However, no significant color changes are observed at the non-specific sites (GOx, A2, A3, B1, B4, C1, C4, D2, D3) and blank control sites (E1-E4). Figure 2d further shows the spectral SPR image after the buffer washing process. No observable color changes were observed in the specific sites. It reveals the specificity of the observed bindings. A complete set of spectral SPR images is shown in Figure S-3 in the supporting information.

As reported in (Ho et al., 2006; Wong et al., 2011; Wong et al., 2008; Wong et al., 2007; Wong et al., 2005), the HSV color space (Smith et al., 1978) has been demonstrated for the color changes quantification in spectral SPR image. HSV color space was introduced by Smith in 1978 (Smith et al., 1978). Hue (H), Saturation (S) and Value (V) are the three dimensions in the HSV color code and the Hue (H) component directly refers to the dominant wavelength of a color (Bose et al., 2004; Heijden et al., 1994). The Hue profile of the spectral SPR images shown in Figure S3a-S3i are extracted with a home built MatLab program and the corresponding 2D Hue maps are shown in Figure 3. In the first 30 minutes of the experiment, the protein array was kept in PBS buffer. Comparing Figure 3a (at the beginning of experiment) and 3b (30mins), average 0.8% variation is found in the specific BSA antigen sites, while 1.0 % and 1.3 % of signal variations are recorded in the non-specific GOx sites and control sites respectively. Figure 3d illustrates the 2D Hue map obtained at 5 minutes after the injection of BSA antibody (2.5µl/ml). The average responses in the specific BSA antigen sites have been increased from 0.19 (hue unit) to 13.95 (hue unit), which is equivalent to 66.2% increase, while less than 3.1 % increase is recorded in the non-specific GOx sites. The 2D Hue profiles obtained at 15 minutes, 30 minutes and 45 minutes after the antibody injection are revealed in Figure 3e, 3f and 3g respectively. As shown in the results, the responses in the specific sites have been increased from 13.95 (hue unit) to 38.52 (hue unit) in 45 minutes. However, relatively less variation is found between Figure 3g (76mins) and 3h (90mins), which is caused by the equilibrium of binding. To remove the non-specific binding on the sensor surface, the array surface was washed with PBS buffer and less

than 1% signal decreases are recorded in the specific sites (Figure 3i). It reveals the specificity of the binding interactions. Comparing the 2D Hue profiles shown in Figure 3i and Figure 3a, average 162.1 % increase is shown in the specific BSA antigen sites, while only 4.45% increases are recorded in the non-specific GOx sites. The imaging experimental results have successfully demonstrated the multiplex, real-time and quantified detection capability of the spectral SPR imaging sensor for array based specific bio-molecular bindings. The observed non-specific binding in the experiment (which is 36 times lower than the response in the specific sites) is caused by the limitation of the current using flow cell in the experiment. A certain portion of non-specific molecules cannot be washed away effectively in the PBS washing procedure after the binding process and these molecules is the cause of the non-specific binding response observed during the experiment. This problem can be solved by using a flow system equipped with automatic mechanical pump, which can provide better washing effect to the sensor surface during the experiment.

The Hue responses in all array elements are further extracted and plotted against time and the corresponding binding curves are shown in Figure 4. Figure 4a, 4d, 4f, 4g, 4j, 4k, 4m and 4p reveal the binding curves of the specific BSA antigen sites, and the binding curves of the non-specific GOx sites are illustrated in Figure 4b, 4c, 4e, 4h, 4i, 4l, 4n and 4o. Figure 4q-4t shows the binding curves of the blank control sites.

The sensor resolution of the spectral SPR imaging sensor can be calculated with the following equation (Homola et al., 2006),

$$Detection \quad Limit = \frac{Concentration \quad of \quad bio-molecule}{Sensor \quad response} \times Measurement \quad Stability \qquad (10)$$

As shown in Figure 4a, 4d, 4f, 4g, 4j, 4k, 4m and 4p, an injection of 2.5μg/ml BSA antibody has produced a response of 39.13 (hue unit) (average value from all specific sensor sites). Table 1 illustrates the measurement stand deviation (S.D.) values recorded in different sensor sites within 30 minutes when the protein array was kept in PBS buffer. The overall measurement S.D. (averaged from all sensor sites responses) is 0.13 (Hue unit), which indicates the measurement

stability of the spectral SPR imaging sensor. From equation 10, the sensor resolution of the system is found to be 8.26 ng/ml (125pM).

Detection experiment on BSA antibody in 97.7 ng/ml concentration has further been carried with the spectral SPR imaging sensor and the BSA antigen-antibody binding curve is shown in Figure S-4 (supplementary materials). The result demonstrates the practical detection capability of the imaging sensor for low concentration bio-molecular samples (in ng/ml), while only calculated detection limit values are given in the literature (Lee et al., 2007; Wong et al., 2008; Wong et al., 2007; Yu et al., 2005; Yu et al., 2008).

Yu *et al.* (Yu et al., 2005) demonstrated the common-path SPR imaging interferometry technique for micro-array detection. The system has been applied for the detection of IgG antibody-antigen binding. However, the sensor responses were relatively noisy. Later on Lee *et al.* (Lee et al., 2007) reported a phase-sensitive SPR imaging system, in which the single beam phase-stepping interferometer (PSI) technique has been employed for the system stability enhancement. The system was integrated with a micro-fluidic platform and the detection of rabbit immunoglobulin G antibody-antigen binding interactions has been demonstrated. The detection limit was found to be 1 x 10^{-4} mg/ml. A differential phase measurement scheme between the p- and s- polarization beam has been demonstrated by Wong *et al.* (Wong et al., 2008; Wong et al., 2007) for SPR imaging. The system has been applied for the detection of BSA antigen- antibody binding. The detection limit was found to be 0.77 μg/ml. In the same year, Yu *et al.* (Yu et al., 2008) presented a SPR imaging system based on the time domain phase modulation interference. For noise suppression, signal averaging among 100 x 100 pixels was required, which reduced the spatial resolution of the phase image. Detection on IgG antigen-antibody binding has been carried. The sensor resolution can be estimated to be ~30 μg/ml (based on phase noise of 0.5°) from the experimental results. As described above, the sensor resolution of our spectral SPR imaging sensor is 8.26 ng/ml. This value is 12.1 times better than the resolution reported in (Lee et al, 2007). Furthermore, it is 93.2 times and 3630.1 times better than that reported in (Wong et al., 2008; Yu et al., 2008) respectively. These results reveal that our polarization orientation based spectral SPR imaging sensor provides significant resolution improvement comparing to existing phase-sensitive SPR imaging sensors based on the common-path SPR imaging interferometry

(Lee et al., 2007), single beam phase-stepping interferometer (PSI) (Yu et al., 2005), differential phase measurement scheme between p- and s- polarization (Wong et al., 2008; Wong et al., 2007) and time domain phase modulation interference (Yu et al., 2008). In addition, area averaging is normally required for noise suppression in phase-sensitive SPR imaging sensors. As reported in (Wong et al., 2008; Wong et al., 2007) and (Yu et al., 2008), area averaging (among 5 x 5 pixels (Wong et al., 2008; Wong et al., 2007) and 100 x 100 pixels (Yu et al., 2008)) is required for phase imaging measurement. It is because that interferometry based phase systems are extremely sensitive to environmental vibrations. Our spectral SPR imaging sensor probes the rotation of the polarization ellipse caused by the phase difference between the p- and s-polarization at SPR with a pair of crossed polarizer. It is not an interferometry based phase detection technique and insensitive to environmental vibrations. Area averaging is not required for the SPR image obtained by our method. It therefore can provide SPR images with higher spatial (2D) resolution comparing to existing phase-sensitive SPR imaging sensors (Yu et al., 2005; Lee et al., 2007; Yu et al., 2008; Wong et al., 2008; Wong et al., 2007). Moreover, no complicated phase modulation process is required, which enhances the response time of the sensor for rapid molecular detection.

4. Conclusion

We have demonstrated a colorimetric surface plasmon resonance (SPR) imaging biosensor array based on polarization orientation. It measures the spectral characteristic variations caused by the steep phase change between the p- and s- polarization component occurring at surface plasmon excitation.

Real-time, multiplexed and quantified detection of specific binding interactions between bovine serum albumin (BSA) antigen-antibody occurring on a protein array have been demonstrated with the spectral SPR imaging sensor. The sensor resolution of the imaging sensor is found to be 8.26 ng/ml (125pM), which is one-order of magnitude (12 times) better than the detection limit reported by existing phase-sensitive SPR imaging sensors in the literature (Yu et al., 2005; Lee et al., 2007; Yu et al., 2008; Wong et al., 2008; Wong et al., 2007) for bioaffinity adsorption measurements. The spectral SPR imaging sensor probes the rotation of the polarization ellipse

caused by the phase difference between the p- and s- polarization at SPR with a pair of crossed polarizers and no complicated phase modulation and phase extraction processes are required. It reduces the data processing time and enhances the sensor temporal resolution for real-time bio-molecular bindings monitoring. Due to the improvement in measurement stability of the system, area averaging which is normally needed for noise suppression in phase-sensitive SPR imaging sensors is not required. It further enhances the sensor spatial resolution for high throughput array detection applications.

The polarization orientation based spectral SPR imaging sensor provides the capability for non-labeling, real-time, quantified and high sensitivity array based analytical detection. It can find promising applications in cancer biomarkers discovery and clinical disease diagnosis.

Acknowledgments
This project is supported by Singapore Bio-Imaging Consortium (SBIC) under grant RPC-015 /2007. Chi Lok Wong would like to thank Jesus for all the grace in this project. Acknowledgment also goes to his mother, Lai Tin Ho, for her consistent support in prayer for the works.

References

Ackermann, B. L., Hale, J. E., Duffin, K. L., 2006. Current Drug Metabolism 7, 525–539.

Addona, T. A., Shi, X., Keshishian, H., Mani, D. R., Burgess, M., Gillette, M. A., Clauser, K. R., Shen, D., Lewis, G. D., Farrell, L. A., Fifer, M. A., Sabatine, M. S., Gerszten, R. E., Carr, S. A., 2011. Nature Biotechnology 29, 635-643.

Angenendt, P., 2005. Drug Discovery Today 10, 503-511.

Bass, M. B., Sherman, S. I., Schlumberger, M. J., Davis, M. T., Kivman, L., Khoo, H. M., Notari, K. H., Peach, M., Hei, Y. J., Patterson, S. D., 2010. The Journal of Clinical Endocrinology & Metabolism 95 (11), 5018-5027.

Bose, T., 2004. Digital signal and image processing, Wiley, New York.

Chandra, H., Reddy, P. J., Srivastava, S, 2011. Expert Rev. Proteomics. 8(1), 61-79.

Choe, L. H., Werner, B. G., Lee, K. H., 2006. NeuroRx Research 3, 327–335.

Cima, I., Schiess, R., Wild, P., Kaelin, M., Schüffler, P., Lange, V., Picotti, P., Ossola, R.,

Templeton, A., Schubert, O., Fuchs, T., Leippold, T., Wyler, S., Zehetner, J., Jochum, W., Buhmann, J., Cerny, T., Moch, H., Gillessen, S., Aebersold, R., Krek, W. 2011. Proceedings of the National Academy of Sciences 108(8), 3342-3347.

Eugene H., 2001. Optics, forth ed., Addison-Wesley, Boston.

Galvão, E. R. C. G. N., Martins, L. M. S., Ibiapina, J. O., Andrade, H. M., Monte, S. J. H., 2011. Journal of Cancer Research and Clinical Oncology 137(6), 915-925.

Gerszten, R. E., Asnani, A., Carr, S. A., 2011. Circulation Research 109, 463-474.

Haab, B. B., Dunham, M. J., Brown, P. O., 2001. Genome Biology 2, research0004.1-0004.13.

Haab, B. B., 2003. Proteomics 3, 2116–2122.

Homola, J., 2008. Chemical Reviews 108 (2), 462–493.

Homola, J., 2006. Surface Plasmon Resonance Based Sensors, Springer-Verlag, Heidelberg.

Homola, J., Yee, S. S., Gauglitz**,** G**.,** 1999. Sensors and Actuators B: Chemical 54**,** 3-15.

Homola, J., Yee, S. S., 1998. Sensors and Actuators B: Chemical 51(1-3), 331-339.

Homola, J., Vaisocherová, H., Dostálek, J., Piliarik, M., 2005. Methods 37(1), 26-36.

Ho, H. P., Wong, C.L., Chan, K.S., Wu S.Y., Lin, C., 2006. Applied Optics 45, 5819-5826.

Ho, H.P., Wong, C.L., Wu, S.Y., Law, W.C., Lin, C. L., Kong, S.K., 2007. Optical Sensing Devices with SPR Sensors Based on Differential Phase Interrogation and Measuring Method Using the Same. U.S. Patent No.US2007/0008546 A1.

Heijden, F. V. D., 1994. Image Based Measurement system, Wiley, New York.

John, S.H., Kenneth, J., Gandhe, A. S., 2012. Biomarkers 17(1), 1-8.

Jordan, C. E., Corn, R. M., 1997. Analytical Chemistry 69, 1449−1456.

Lam, W. W., Chu, L. H., Wong C. L., Zhang, Y. T., 2005. Sensors and Actuators B: Chemical 105(2), 138-143.

Lee, H. J., Nedelkov, D., Corn, R. M., 2006. Analytical Chemistry 78 (18), 6504–6510.

Lee, H. J., Wark, A. W., Corn, R. M., 2008. Analyst 133, 975-983.

Lee, K. H., Su, Y. D., Chen, S. J., Tseng, F. G., Lee, G. B., 2007. Biosensors and Bioelectronics 23(4), 466-472.

Matarraz, S., González-González, M., Jara, M., Orfao A., Fuentes, M., 2011. Clinical and Translational Oncology, 13(3), 156-161.

Mor, G., I., Visintin, Y., Lai, H. Zhao, Schwartz, P., Rutherford, T., Yue, L., Bray-Ward, P., Ward, D. C., 2005. Proceedings of the National Academy of Sciences 102, 7677–7682.

Motoki, K., Kazue, U. A., Hisashi, K., 2005. Analytical Chemistry 77 (22), 7115–7121.

Natesan, M., Ulrich, R. G., 2010. International Journal of Molecular Sciences 11(12), 5165-5183.

Nelson, B. P., Frutos, A. G., Brockman, J. M., Corn, R. M., 1999. Analytical Chemistry 71, 3928−3934.

Nelson, S. G., Johnston, K. S., Yee, S. S., 1996. Sensors and Actuators B: Chemical 35-36, 187-191.

Peña, C., Lathia, C., Shan, M., Escudier, B., Bukowski R. M., 2010. Clinical Cancer Research 16, 4853-4863.

Rothenhausler, B., Knoll, W., 1998. Nature 332, 615 - 617.

Rucker, V. C., Havenstrite, K. L., Herr, A. E., 2005. Analytical Biochemistry 339, 262-270.

Sanchez-Carbayoa M., 2006. Clinical Chemistry (Washington, D. C.) 52, 1651–1659.

Schaaij-Visser, T. B. M., Brakenhoff, R. H., Leemans, C. R., Heck, A. J. R., Slijper, M., 2010. Journal of proteomics 73(10), 1790-1803.

Shi, M., Bradner, J., Hancock, A. M., Chung, K. A., Quinn, J. F., Peskind, E. R., Galasko, D., Jankovic, J., Zabetian, C. P., Kim, H. M., Leverenz, J. B., Montine, T. J., Ginghina, C., Kang, U. J., Cain, K. C., Wang, Y., Aasly, J., Goldstein, D., Zhang J., 2011. Annals of Neurology, 69(3), 570-580.

Smith, A.R., 1978. Computer Graphics 12(3), 12-19.

Surinova, S., Schiess, R., Hüttenhain, R., Cerciello, F., Wollscheid, B., Aebersold, R., 2011. Journal of Proteome Research 10 (1), 5–16.

Tomizaki, K. Y., Usui, K., Mihara, H., 2010. FEBS Journal 277(9), 1996-2005.

Wong, C. L., 2007. Imaging surface plasmon resonance (SPR) photonic sensors, Thesis (Ph.D.), The City University of Hong Kong, Hong Kong.

Wong, C. L., Ho, H. P., Chan, K. S., Wong, P. L., Wu, S.Y., Guo F., Lin, C., 2008. Tribology International 41 (5), 356-366.

Wong, C.L., Ho, H.P., Chan, K.S., Wu, S.Y., 2005. Applied Optics 44, 4830-4837.

Wong, C. L., Ho, H. P., Chan, K. S., Wu, S. Y., Lin, C., 2005. Optical Engineering 44, 124403.

Wong, C. L., Ho, H.P., Suen, Y.K., Kong, S.K., Chen, Q.L., Yuan, S. W., Wu, Y., 2008. Biosensors and Bioelectronics 24 (4), 606-612.

Wong, C. L., Ho, H. P., Yu, T. T., Suen, Y. K., Chow, W. W. Y., Wu, S. Y., Law, W. C., Yuan,

W., Li, W. J., Kong, S. K., Lin, C., 2007. Applied Optics 46, 2325-2332.

Wong, C.L., Yu, X., Shum, P., Ho, H.P., 2011. Optical Characterization of Elastohydrodynamic Lubrication Pressure with Surface Plasmon Resonance, in: Ghrib, T. (Ed.), New Tribological Ways, Intech, Rijeka, pp. 21-45.

Yeatman, E., Ash, E., 1987. Electronics Letters 23, 1091–1092.

Yu, X. L., Ding, X., Liu, F. F., Deng, Y., 2008. Sensors and Actuators B: Chemical 130(1), 52-58.

Yu, X. L., Wang, D. X., Wei X., Ding X., Liao W., Zhao X. S., 2005. Sensors and Actuators B: Chemical 108(1-2), 765-771.

Yuk, J. S., Jung, J. W., Hyun, J., Kim, Y. M., Ha, K. S., 2008. Sensors and Actuators B: Chemical 131 (1), 241-246.

Yuk, J. S., Lee, M. J., Kim, U. R., Ha, K. S., 2007. Current Applied Physics (1), 102-107.

Yuk, J. S., Yi, S. J., Lee, H. G., Lee, H. J., Kim, Y. M., Ha, K., 2003. Sensors and Actuators B: Chemical 94(2), 161-164.

Table 1 Measurement stand deviation (S.D.) values of different sensor sites within 30 minutes, when the protein array was kept in PBS buffer. The overall measurement S.D. (averaged from all sensor sites responses) is 0.13 (Hue unit), which indicates the measurement stability of the spectral SPR imaging sensor.

Sensor site location	**A1**	**A2**	**A3**	**A4**	**B1**	**B2**	**B3**	**B4**
Measurement S.D. (Hue unit)	0.16	0.08	0.11	0.10	0.12	0.09	0.10	0.14
Sensor site location	**C1**	**C2**	**C3**	**C4**	**D1**	**D2**	**D3**	**D4**
Measurement S.D. (Hue unit)	0.19	0.15	0.17	0.18	0.16	0.19	0.16	0.18
Sensor site location	**E1**	**E2**	**E3**	**E4**				
Measurement S.D. (Hue unit)	0.07	0.09	0.10	0.06				
0.5								
Averaged overall measurement S.D.	0.13 (Hue unit)							

List of captions

Figure 1 a) Ellipse of the elliptically polarized light E' b) Schematic diagram of the polarization orientation based spectral SPR imaging sensor. c) The protein array consists of 3 different array elements: bovine serum albumin (BSA) (red spots, positive sample), glucose oxidase (GOx) (black spots, negative sample) and blank sites (white spots, background control) d) Representative spectral SPR image taken when the array was kept in PBS buffer before the experiment (averaged with 10 images) (the scale bar represents 1mm in length).

Figure 2 Spectral SPR images for specific BSA antigen-antibody binding detection (the scale bar represents 1mm in length) a) at the beginning of the experiment, the protein array was kept in PBS buffer. b) (46mins) 15 minutes after the injection of anti-BSA. c) (90mins) 1 hour after the injection of BSA antibody. d) (106mins) 15 minutes after the PBS buffer washing process.

Figure 3 2D hue profiles extracted from the spectral SPR images (for normalization propose, images are subtracted with the representative spectral SPR image shown in Figure S-2, which was taken when the protein array was in PBS buffer and the scale bar represents 1mm in length) a) at the beginning of the experiment, the array was kept in PBS buffer. b) (30mins) the array was kept in PBS buffer. c) (32mins) 1 minute after the injection of anti-BSA (2.5µl/ml in PBS). d) (36mins) 5 minutes after the injection of anti-BSA. The average response in the specific BSA antigen sites is increased from 0.19 (hue unit) to 13.95 (hue unit), which is equivalent to 66.21% increase. However, less than 3.05 % increases are recorded in the non-specific GOx sites. e) (46mins) 15 minutes after the injection of anti-BSA. f) (61mins) 30 minutes after the injection of anti-BSA. g) (76 mins) 44 minutes after the injection of anti-BSA. h) (90mins) 59 minutes after the injection of anti-BSA. i) (105mins) 15 minutes after array surface washing with PBS buffer. Less than 1% signal decrease is recorded in the specific sites (Figure 3i). It reveals the specificity of the binding interactions. Comparing the 2D Hue profiles shown in Figure 3i and Figure 3a, 162.1 % increase is found in the specific BSA antigen sites, while only 4.45% increase is indicated in the non-specific GOx sites.

Figure 4 Binding curves for all sensor sites in the array. Figure 4a, 4d, 4f, 4g, 4j, 4k, 4m and 4p reveal the binding curves of the specific BSA antigen sites, and the binding curves of the non-specific GOx sites are illustrated in Figure 4b, 4c, 4e, 4h, 4i, 4l, 4n and 4o. Specific bindings are clearly shown in the specific BSA antigen sites (A1, A4, B2, B3, C2, C3, D1, D4), while less than 5% variations are recorded in the non-specific GOx sites (A2, A3, B1, B4, C1, C4, D2, D3).. At the equilibrium stage, the average response recorded in the specific BSA antigen sites is 24.8 times higher than that of the non-specific GOx sites. In addition, it is 6.2 times higher than that of the blank control sites (Figure 4q-4t, E1-E4).

Table 1 Measurement stand deviation (S.D.) values of different sensor sites within 30 minutes, when the protein array was kept in PBS buffer. The overall measurement S.D. (averaged from all sensor sites responses) is 0.13 (Hue unit), which indicates the measurement stability of the spectral SPR imaging sensor.

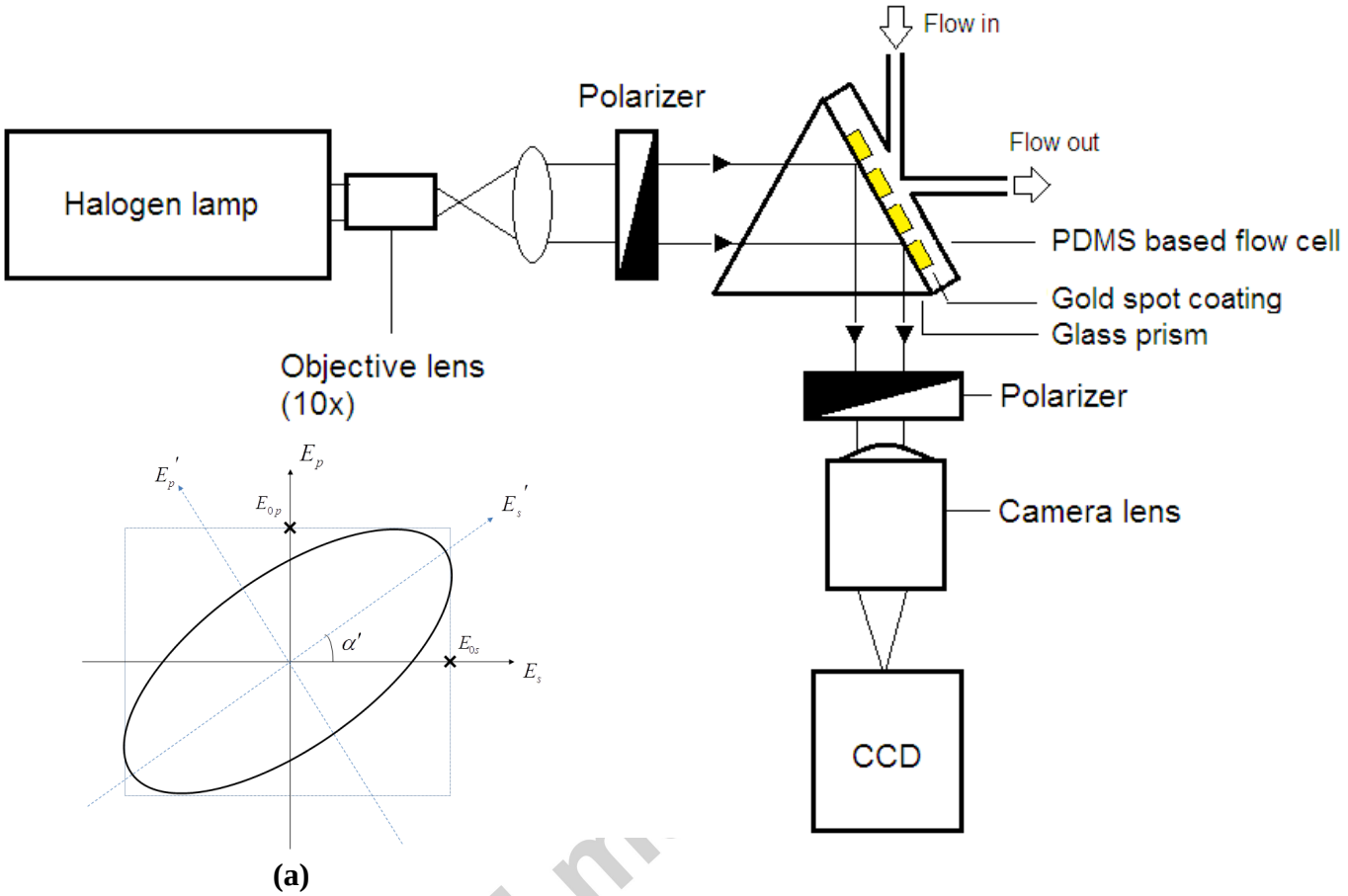
Flow in
Polarizer
Flow out
Halogen lamp
PDMS based flow cell
Gold spot coating
Glass prism
Objective lens
(10x)
Polarizer
Camera lens
CCD
E_p
E_p'
E_{0p}
E_s'
α'
E_{0s}
E_s

(a) **(b)**

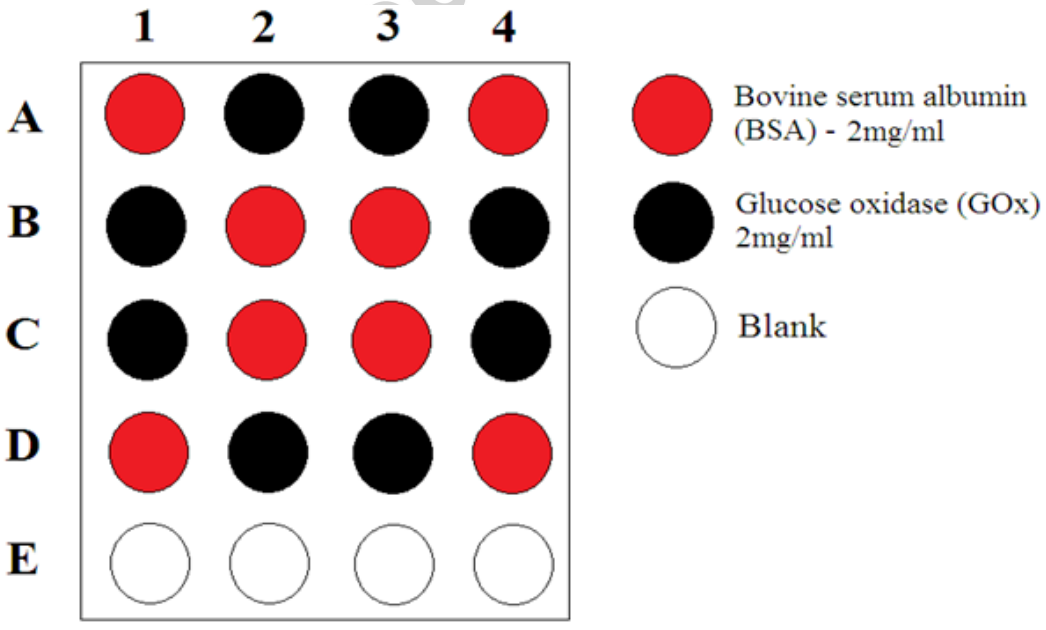
1
2
3
4
A
B
C
D
E
Bovine serum albumin (BSA) - 2mg/ml
Glucose oxidase (GOx) 2mg/ml
Blank

(c)

Figure 1

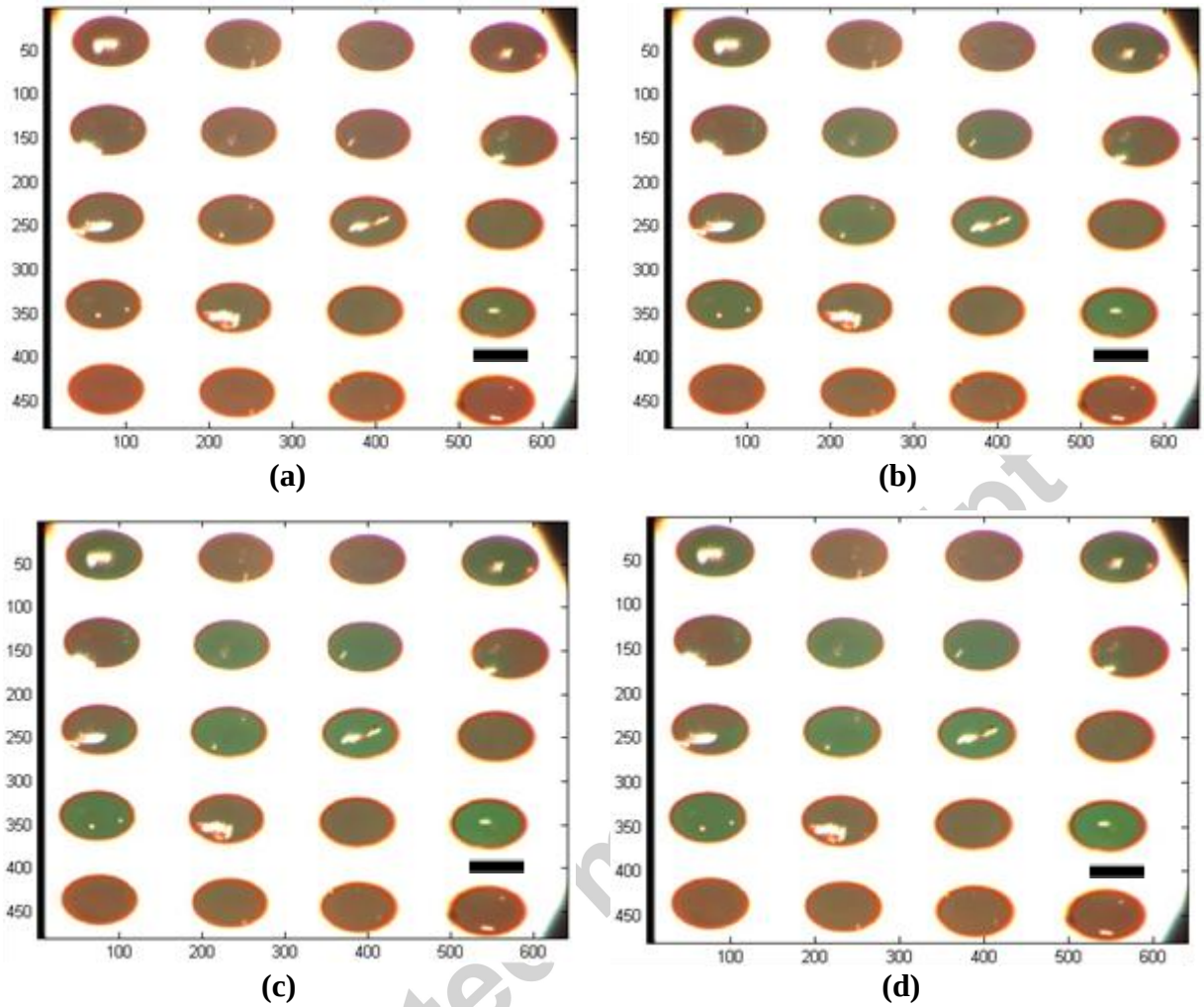

Figure 2

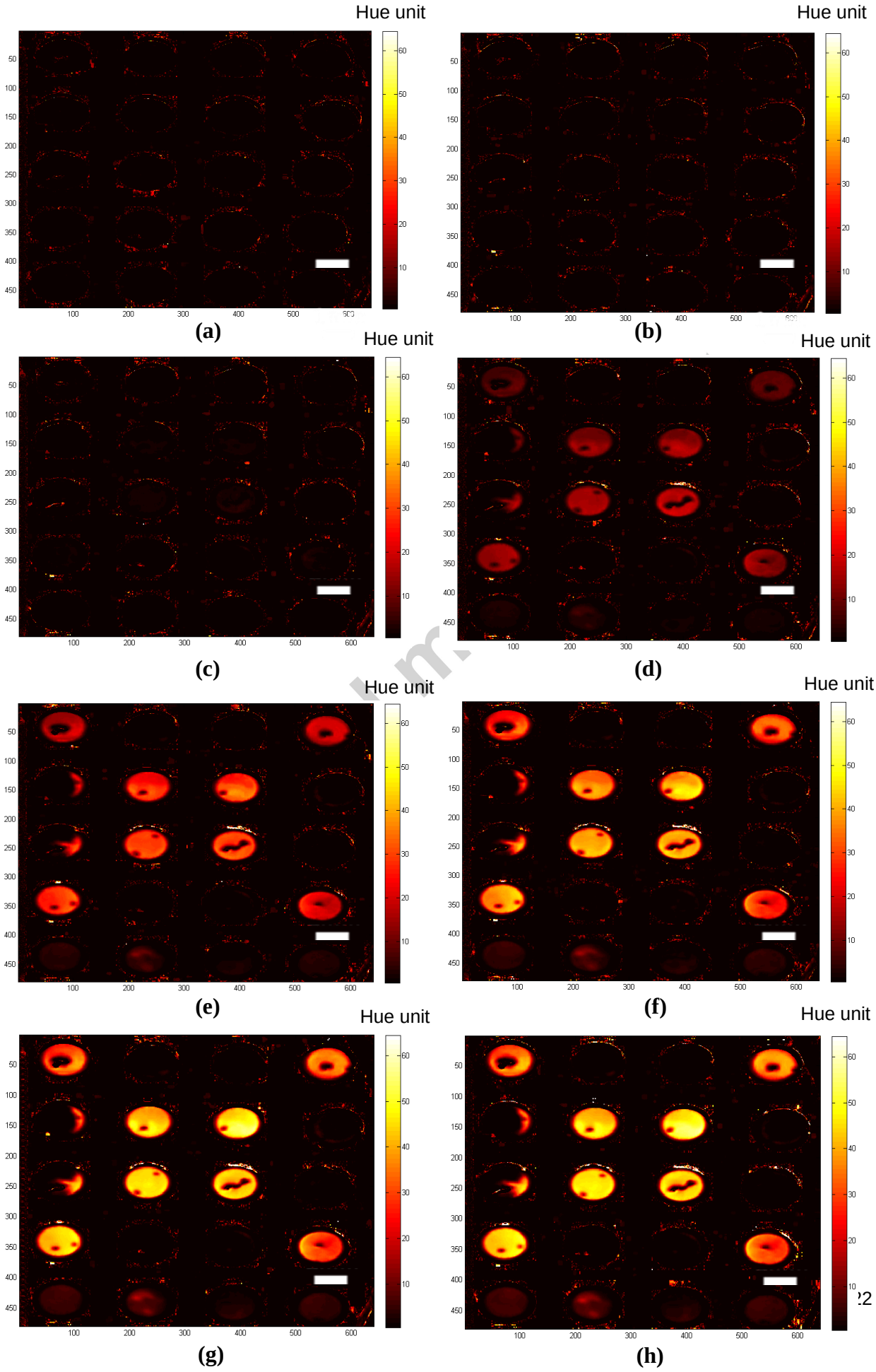

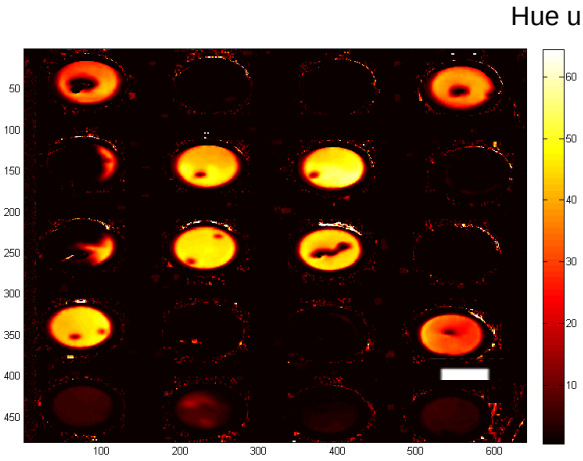

(i)

Figure 3

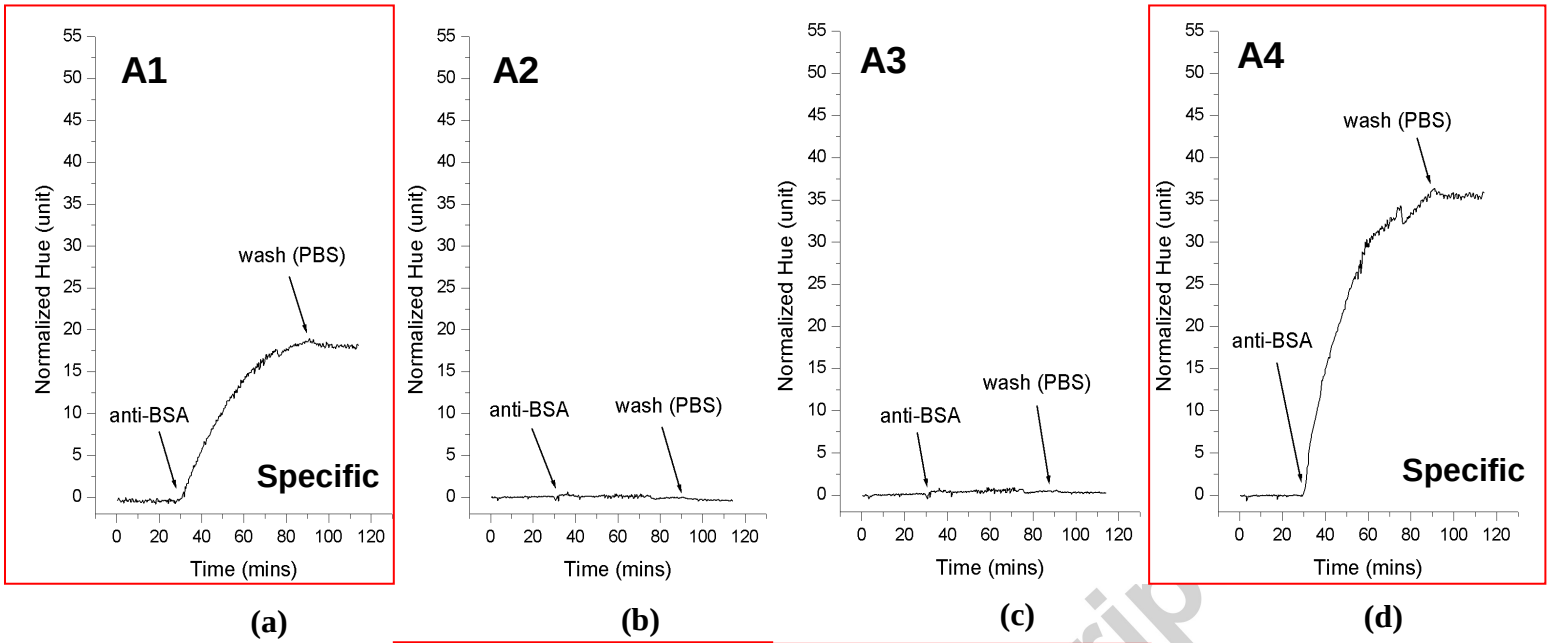

(a) (b) (c) (d)

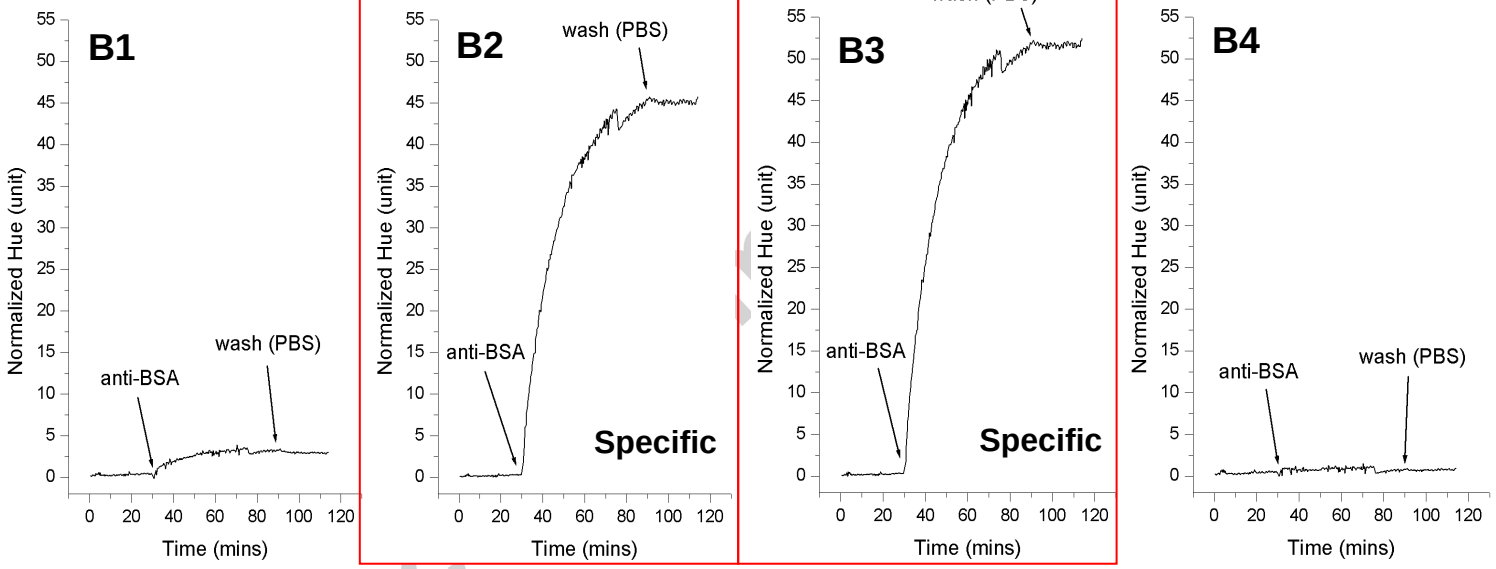

(e) (f) (g) (h)

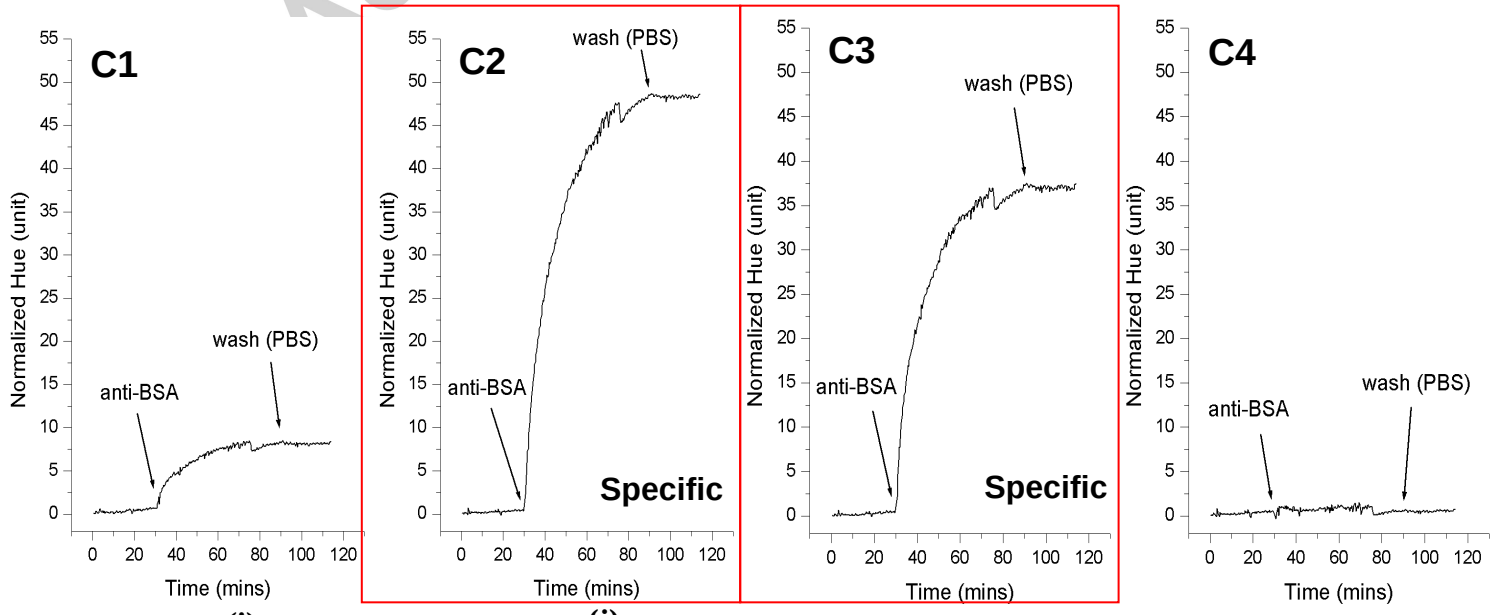

(i) (j) (k) (l)

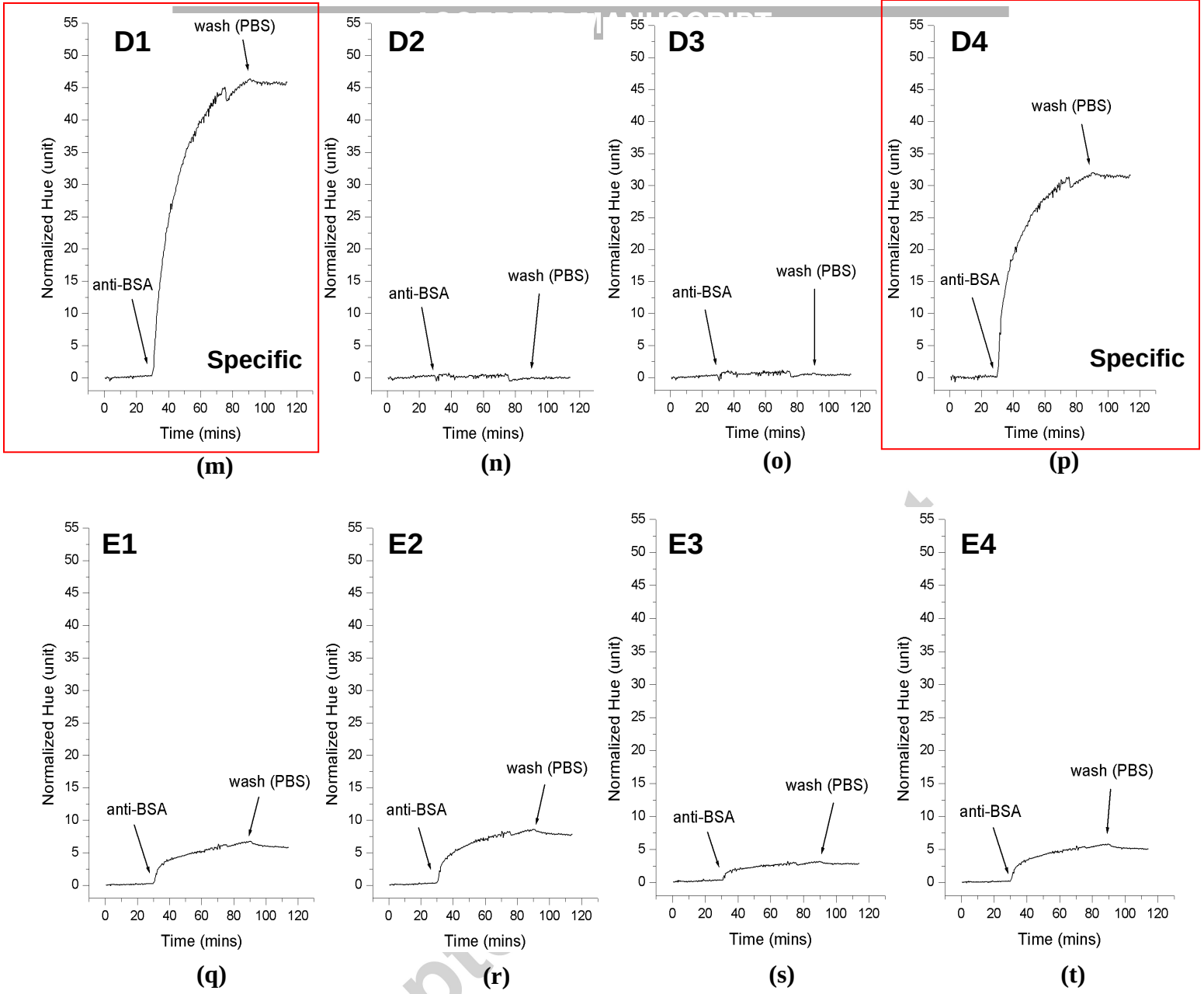

Figure 4